System Level Modeling and Optimization of the Polar Coordinate Detector for Laser Guide Star Adaptive Optics Wavefront Sensing

Sean M. Adkins, Sandrine Thomas, Don Gavel

CfAO Fall Retreat Presentation
November 17, 2006

Project Structure

- CfAO funding to look at system level issues related to the design of the "phase 2" device from an Adaptive Optics Development Program (AODP) funded project:

"Development of the Next Generation Optical Detectors for Wavefront Sensing"

Sean Adkins, James W. Beletic, Barry Burke, Charlie Bleau, Ray DuVarney,
Jerry Nelson, Richard Stover and Francois Rigaut

AODP Project Objectives

- Develop 2 new wavefront sensors for adaptive optics
- Phase 1, now the CCID-56
    - Goal is a very low noise detector for a Shack-Hartmann wavefront sensor
    - Planar JFET output structure
    - 20 video outputs, ~ 1 MHz maximum pixel rate per output
    - 160 x 160 pixels
    - Demonstrated read noise of < 1 e-
- Phase 2, a “polar coordinate detector” soon to be the CCID-??

W. M. KECK OBSERVATORY

Polar Coordinate Detector

- CCD optimized for LGS AO wavefront sensing on an Extremely Large Telescope (ELT)
  - Allows good sampling of a CW LGS image along the elongation axis
  - Allows tracking of a pulsed LGS image
  - Rectangular "pixel islands" in each subaperture

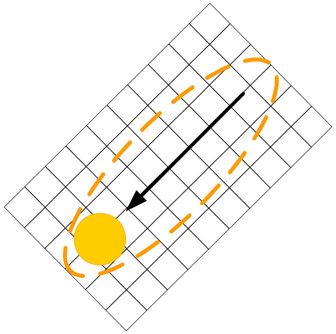

  - Major axis of each rectangle aligned with axis of elongation in that subaperture

Design Questions

- How many pixels?
  - Sampling
  - Dynamic range
- What performance?
  - Frame rate
  - Read noise
- Operating conditions?
  - LGS return flux
    - An intensity distribution = the information content
  - LGS image size
  - LGS Elongation
  - Tilt offsets
  - Seeing

W. M. KECK OBSERVATORY

Current Simulation Work

- Coordinate subaperture level simulation efforts with TMT LGS AO system level simulations

- Take into account system level issues
  - Laser performance
  - Uplink performance
  - Rayleigh scattering
  - Sodium layer variability
  - Non-common path errors
  - Closed and open loop operation

- Adding elongation and sodium layer variability to existing simulations developed by Sandrine Thomas (Thomas et al., MNRAS, 2006)
  - Refine understanding of required wavefront sensor dynamic range
  - Verify optimal sampling
  - Look at potential benefits of pulsed laser with spot tracking compared to CW laser
  - Look at potential benefits of correlation tracking using sodium layer profiles

W. M. KECK OBSERVATORY

Centroid calculation methods

✓ CoG:
  - Windowing, W
  - Weighted CoG, F_w

$$C_x = \alpha \frac{\sum_{i,j} x_i I_{i,j} F_{w,i,j}}{\sum_{i,j} I_{i,j}}$$

✓ Correlation

$$F_{corr}(x,y) = I \otimes F_w = \sum_{i,j} I_{i,j} F_w(x_i + x, y_i + y)$$

Correlation peak estimation:

- CoG + thresholding, T
- Parabola fitting (Poyneer, 2003)
- Gaussian fitting

CoG

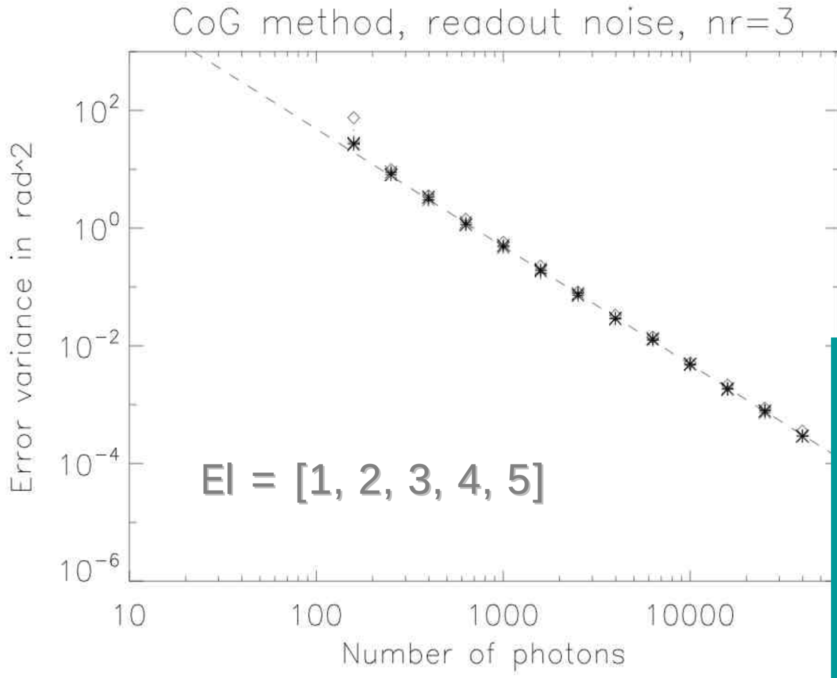

σ^2_{ron} depends only on the number of pixels

$$\boxed{\sigma^2_{ron,x} = \frac{\pi^2}{3}\frac{N_r^2}{N_{ph}^2}\frac{N_{sx}^3 N_{sy}}{N_D^2}}$$

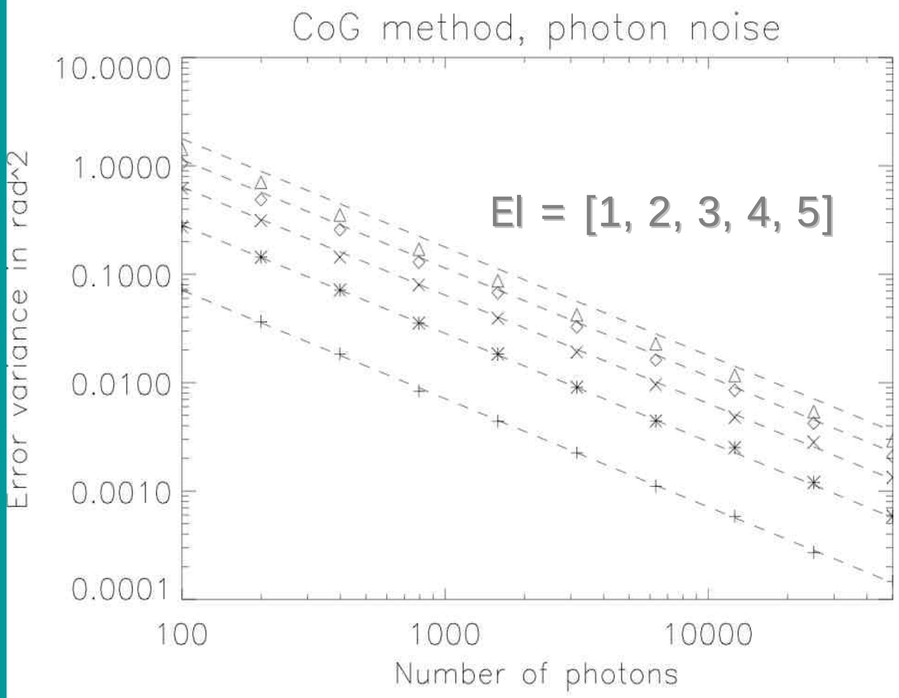

σ^2_{Nph} is proportional to el^2

$$\boxed{\sigma^2_{Nph,x} = \frac{\pi^2}{2\ln 2}\frac{1}{N_{ph}}\frac{N_{Tx}^2}{N_D^2}}$$

W. M. KECK OBSERVATORY

Weighted windowing

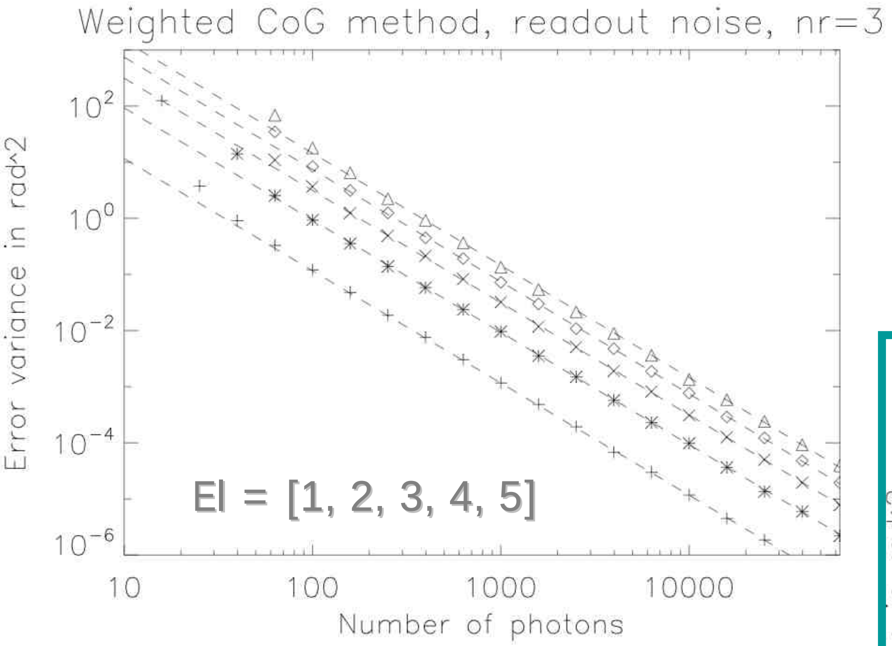

σ^2_{ron} is proportional to el^3

$$\sigma^2_{ron,x} = \frac{\pi^3}{32(\ln 2)^2}\frac{N_r^2}{N_{ph}^2}\frac{\left(N_{wx}^2+N_{tx}^2\right)^3\left(N_{wy}^2+N_{ty}^2\right)}{N_{wx}^3 N_{wy} N_D^2}$$

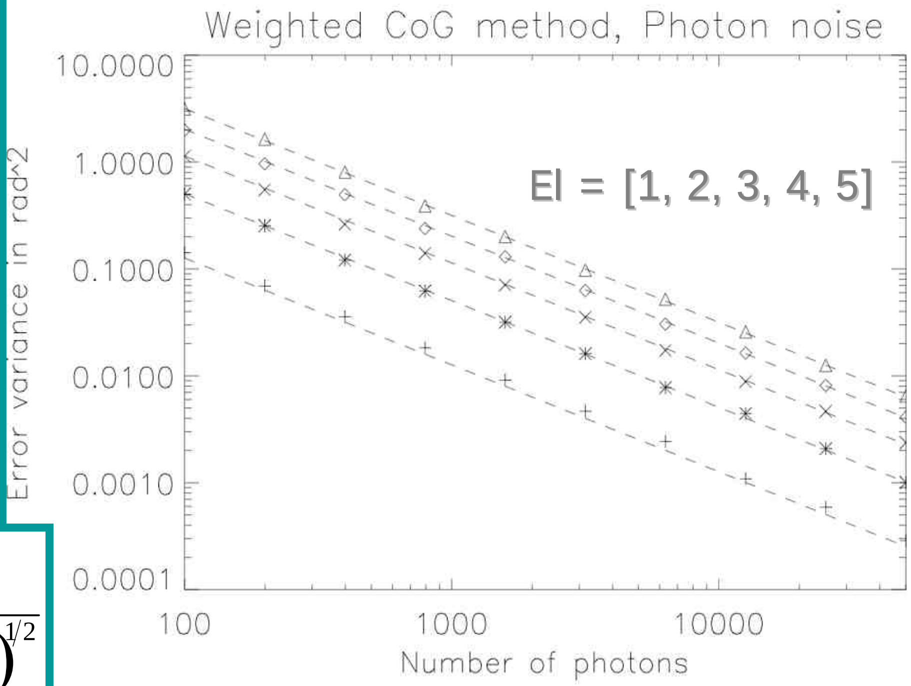

σ^2_{Nph} is proportional to el^2

$$\sigma^2_{Nph,x} = \frac{\pi^2}{2(\ln 2)}\frac{1}{N_{ph}^2}\frac{N_{Tx}^2}{N_{wx}^3 N_{wy} N_D^2}\frac{\left(N_{wx}^2+N_{tx}^2\right)^3\left(N_{wy}^2+N_{ty}^2\right)}{\left(N_{wx}^2+2N_{tx}^2\right)^{3/2}\left(N_{wy}^2+2N_{ty}^2\right)^{1/2}}$$

Correlation

Peak determined by thresholding

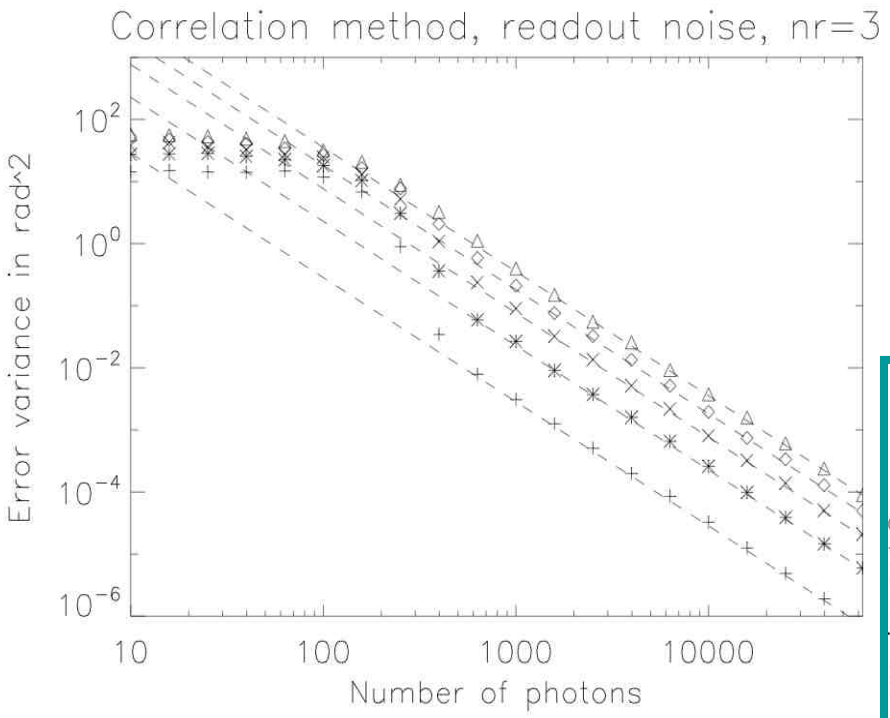

σ^2_{ron} is proportional to el^2

$$\sigma^2_{ron,x} = \frac{\pi^2}{N_D^2}\frac{N_{Tx}N_{Ty}N_r^2}{N_{ph}^2}\left(N_{Tx}^2 + N_{wx}^2\right)$$

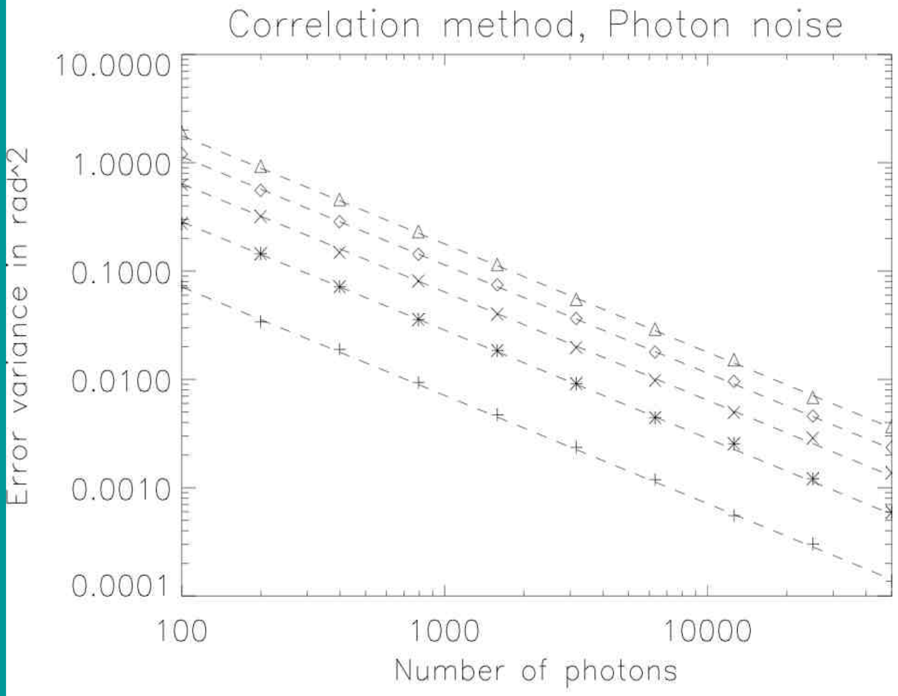

Same as CoG

$$\sigma^2_{Nph,x} = \frac{\pi^2}{2\ln 2}\frac{1}{N_{ph}}\frac{N_{Tx}^2}{N_D^2}$$

Elongation and Sampling

- 10000 photons, readout noise = 3 electrons
- Reference for correlation is identical to the image

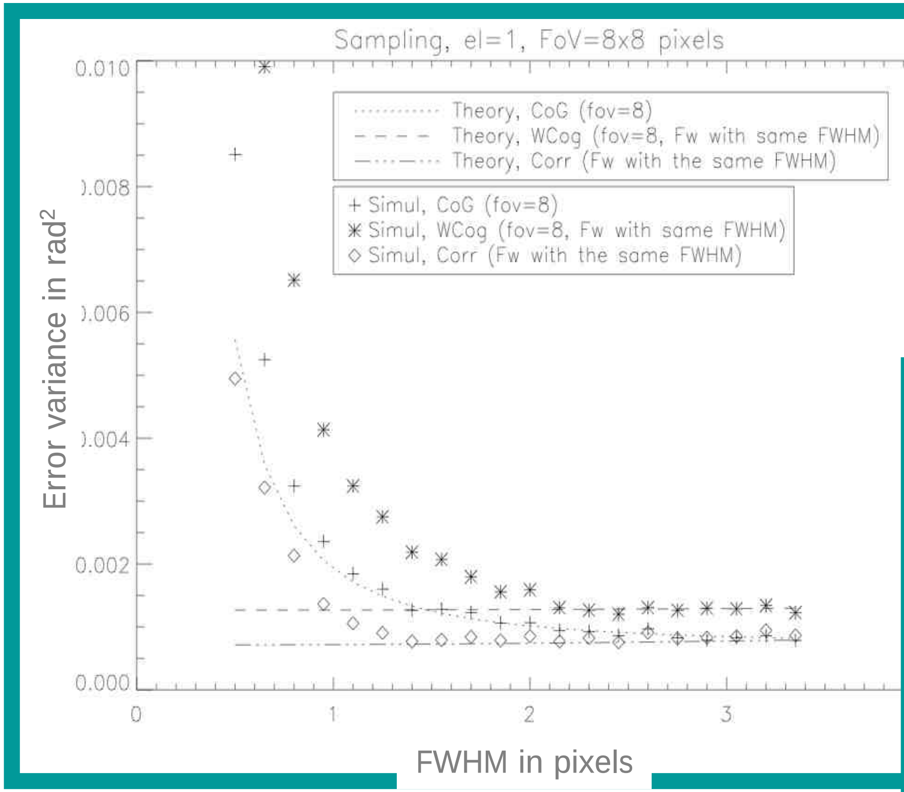

El = 1 or non-elongated direction

El = 4 (Elongated direction)

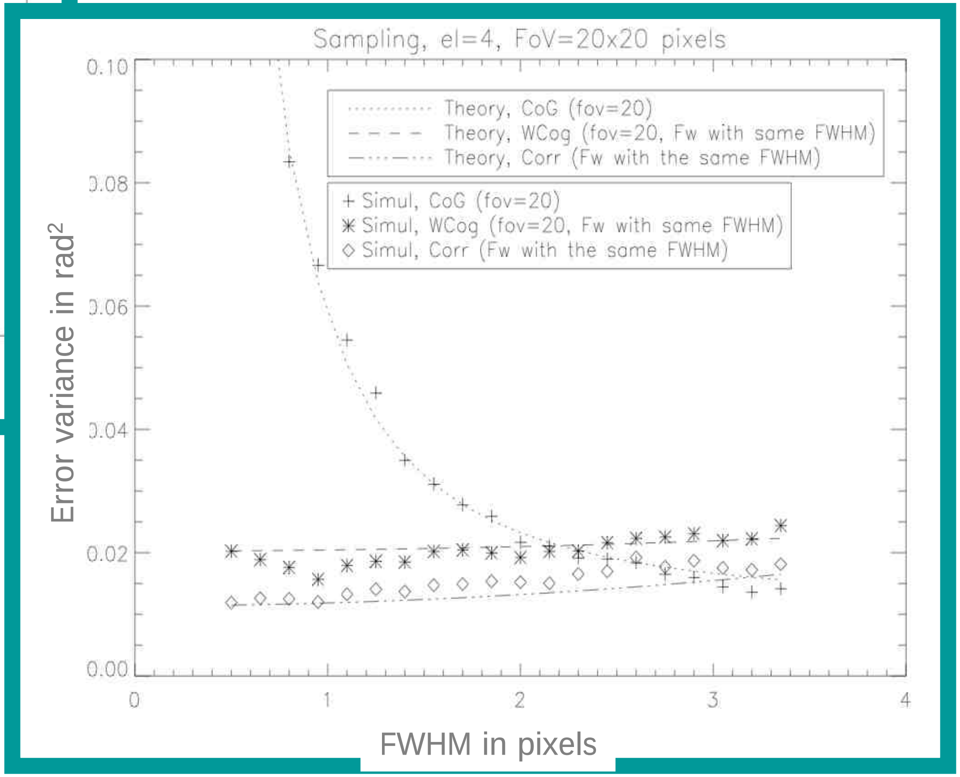

Conclusions and Future work

- Define the optimum sampling with all the error sources (elongation, atmosphere, Rayleigh back-scatter…)
- Give the final wavefront error to Luc Gilles and Brent Ellerbroek to feed LAOS.
- This will finalize the size of the imager array in each subaperture and inform decisions about needed read noise performance and expected photon levels

AODP Phase 2 Design Goals

- Works with both CW and pulsed lasers
- One quadrant of a 60 x 60 subaperture configuration
  - 30 x 30 with 675 active subapertures
  - 8 x 20 pixel imager in each subaperture
  - 10 sets of imager clocks arranged in consecutive rings to permit pulse tracking
  - 34 video outputs for ~20 subapertures each
  - Subapertures on 500 µm pitch
  - ~10 to 12 µm pixels
- Minimum frame rate 800 Hz, goal frame rate 1500 Hz
- Read noise goal of < 2 e-

CCD Issues

- Things the CCD will do well:
  - No significant charge diffusion
  - Excellent CTE
  - Good QE (>80%)
  - Essentially no dark current (op. temp. and frame rate)
  - Very low read noise (< 2 electrons)
  - Good uniformity, 100% operability
- Things to worry about:
  - Pixel clock rate
  - There will be a large number of readout ports
  - The data volumes will be high

Phase 2 Design Status

- Multiplexing vs. long shift registers
  - Output amplifier per subaperture raises power dissipation concerns
  - Multiplexer addressing delay a headache
  - Returning to original concept of a long shift register connecting a set of (~20) subapertures to a single output amplifier

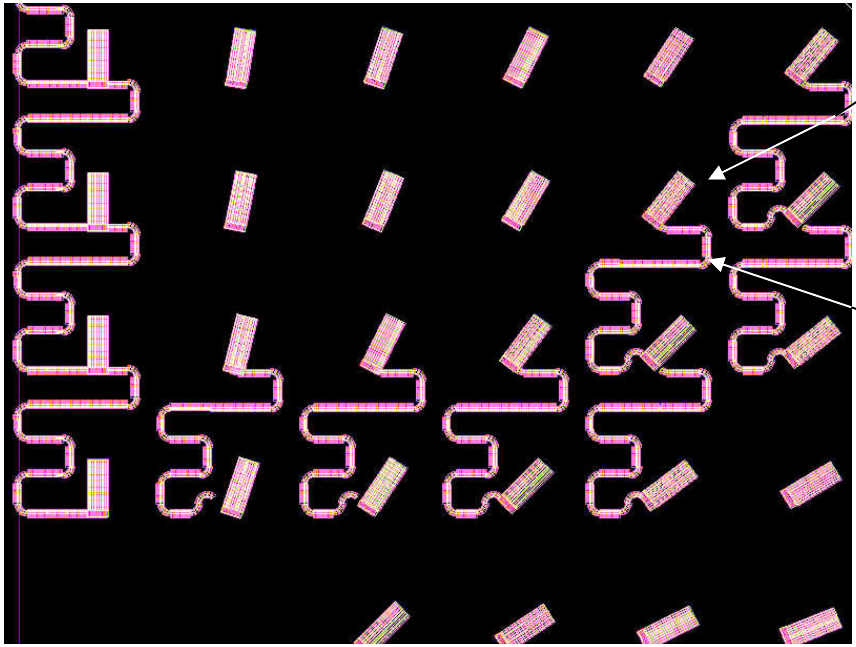

Partial layout example

Subaperture pixel island

Long shift register

Phase 2 Design Status

- Each section of long shift register equal to the number of pixels in a subaperture
- Planning to use on-chip clock divider for annular clock rings needed for pulse tracking
  - On chip NMOS logic followed by level shifter to drive CCD phases – innovation from PANStarrs OTA detectors
- Pin count per quadrant will be reduced, may make entire device realizable using a conventional CCD process
  - Phase 2 device may be much closer to full scale TMT device
  - Lower development risk
- Also considering optimizing pixels per subaperture in each annular ring, fewer pixels in the inner subapertures
  - Improves overall performance by eliminating need to clock unused pixels

Acknowledgements

The TMT Project Office: Brent Ellerbroek, Luc Gilles

Herzberg Institute of Astrophysics: Glen Herriot

The Center for Adaptive Optics

This material is based upon work supported by AURA through the National Science Foundation under AURA Cooperative Agreement AST 0132798, Scientific Program Order No. 6 (AST-0336888) as amended.